Supplementary Information

Single-Molecule Transport of Fullerene-based Curcuminoids

Diana Dulić,[a*] *Alfredo Rates,*[a,c] *Edison Castro,*[b] *Jacqueline Labra-Muñoz,*[a] *Daniel Aravena,*[d] *Alvaro Etcheverry-Berrios,*[e] *Daniel Riba-López,*[f] *Eliseo Ruiz,*[g] *Núria Aliaga-Alcalde,*[f,h] *Monica Soler,*[e] *Luis Echegoyen,*[b] and *Herre S. J. van der Zant*[c*]

a) Department of Physics and Department of Electrical Engineering, Faculty of Physical and Mathematical Sciences, University of Chile, Avenida Blanco Encalada 2008, Santiago 8330015, Chile.
b) Department of Chemistry, University of Texas, 500 West University Avenue, El Paso, Texas 79968, United States.
c) Kavli Institute of Nanoscience, Delft University of Technology, Lorentzweg 1, Delft 2628 CJ, The Netherlands.
d) Department of Material Chemistry, Faculty of Chemistry and Biology, University of Santiago of Chile, Casilla 40, Correo 33, Santiago 9170022, Chile.
e) Department of Chemical Engineering, Biotechnology and Materials, Faculty of Physical and Mathematical Sciences, University of Chile, Beauchef 851,Santiago, 837.0415, Chile.
f) Institut de Ciència de Materials de Barcelona (CSIC-ICMAB), Campus de la Universitat Autònoma de Barcelona, 08193 Bellaterra, Spain.
g) Departament de Química Inorgànica i Orgànica and Institut de Recerca de Química Teòrica i Computacional, Universitat de Barcelona, Diagonal 645, 08028 Barcelona, Spain.
h) ICREA (Institució Catalana de Recerca i Estudis Avançats), Passeig Lluís Companys 23, 08010 Barcelona, Spain.

*Email: ddulic@gmail.com, h.s.j.vanderzant@tudelft.nl

Table of contents:

1. Synthesis and characterization

Recently, some of us described the synthesis of a family of fullerocurcuminoid systems with different curcuminoid motifs attach to the C_{60} cage, which includes CCM-C_{60}.[1] Here the approach was the opposite, fixing now the CCM and exploring the synthesis using different fullerene derivatives.

Regarding the characterization, we focused on the hybridization and changes in the nature of the central C atom of the diarylheptanoid chain of the CCM caused by the different fullerenes. For that, room temperature ^{13}C NMR technique (Figs. S2, S4 and S6) was a useful tool allowing direct comparison between the three systems and the free CCM. The spectra displayed clear shifts from 102.1 ppm, in the case of the free CCM, to 74.1, 68.1 and 72.5 ppm, for the CCM-C_{60}, CCM-C_{70} and CCM-C_{60}P, respectively, matching well with what it is expected for C atoms with sp^2 (free CCM) and sp^3 (fullerocurcuminoids) hybridization, and modifying the conjugation of the final systems.

General Methodology

All chemicals were reagent grade, purchased from Sigma Aldrich. Silica gel (40-60 μ, 60 Å) was used to purify the products from the pristine fullerene. MALDI-TOF mass spectrometry was conducted on a Bruker Microflex LRF mass spectrometer, positive mode, matrix THA and TPB. NMR spectra were recorded using a Bruker 400 MHz spectrometer and JOEL 600 MHz spectrometer.

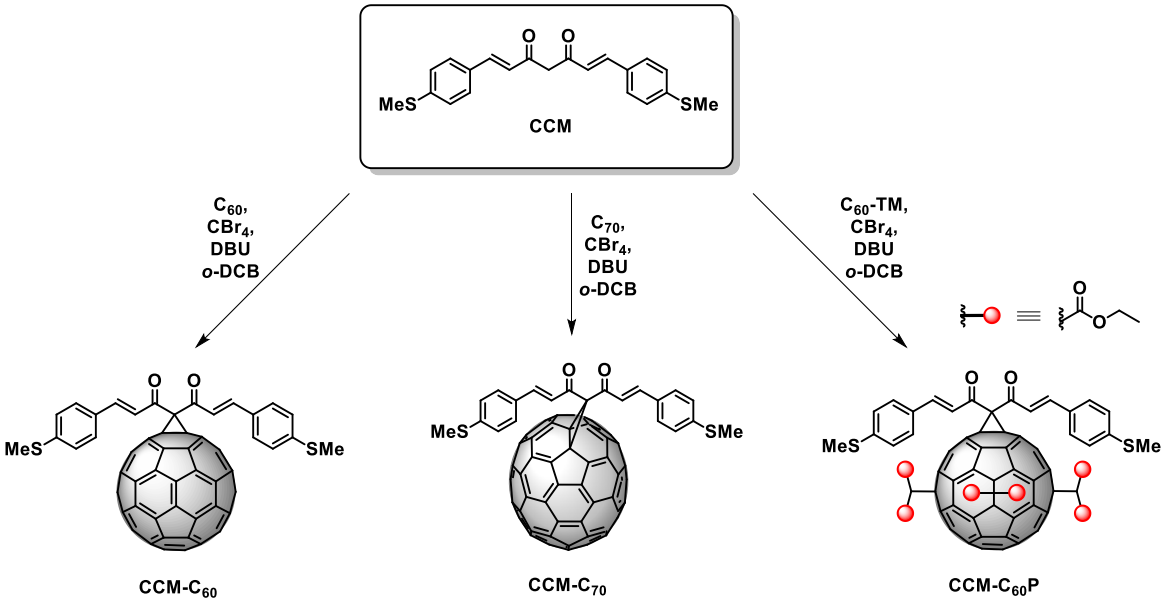

Scheme S1. Synthesis of CCM-C_{60}, CCM-C_{70} and CCM-C_{60}P.

Synthesis of CCM. CCM was synthesized following a procedure previously reported.[2]

Synthesis of CCM-C_{60}: To a solution of 72 mg of C_{60} (0.1 mmol, 1 eq), **CCM** (31 mg, 0.1 mmol, 1eq) and tetrabromomethane (33 mg, 0.1 mmol, 1 eq) in 10 mL of *o*-DCB, was added DBU (2 drops) and stirred at room temperature for 20 min and poured into a silica gel column to stop the reaction and to purify compound **CCM-C_{60}**. Initially, CS_2 was used to recover the unreacted C_{60}, followed by CS_2:$CHCl_3$ 1:1 to recover **CCM-C_{60}** (50% yield). ^{1}H-NMR (600 MHz; $CDCl_3$, 298

K); δ 8.33 (d, 1H), 7.66 (d, 2H), 7.36 (d, 2H), 7.30 (d, 2H), 2.55 (s, 3H) ppm. ^{13}C-NMR (150 MHz; $CDCl_3$, 298 K); δ 186.2, 148.2, 145.9, 145.5, 145.2, 144.7, 144.6, 144.5, 143.8, 143.0, 142.2, 142.2, 141.2, 137.8, 130.2, 130.1, 129.7, 125.8, 122.0, 74.1, 67.9, 15.0 ppm. $C_{81}H_{18}O_2S_2$, m/z calc. 1086.076, found 1086.073.

Synthesis of CCM-C_{70}: To a solution of 84 mg of C_{70} (0.1 mmol, 1 eq), **CCM** (31 mg, 0.1 mmol, 1eq) and tetrabromomethane (33 mg, 0.1 mmol, 1 eq) in 10 mL of *o*-DCB, was added DBU (2 drops) and stirred at room temperature for 25 min and poured into a silica gel column to stop the reaction and to purify compound **CCM-C_{70}**. Initially, CS_2 was used to recover the unreacted C_{60}, followed by CS_2:$CHCl_3$ 1:1 to recover **CCM-C_{70}** (45% yield). ^{1}H-NMR (400 MHz; $CDCl_3$, 298 K); δ 8.29 (d, 2H), 7.68 (d, 4H), 7.31 (d, 4H), 7.30 (d, 2H), 2.56 (s, 6H) ppm. ^{13}C-NMR (100 MHz; $CDCl_3$, 298 K); δ 186.0, 155.6, 151.9, 151.4, 151.2, 150.8, 150.6, 149.4, 149.2, 149.1, 148.5, 148.5, 147.7, 147.5, 147.3, 146.9, 146.4, 145.9, 145.9, 145.1, 144.7, 144.00, 143.8, 143.5, 143.5, 142.7, 141.6, 141.1, 139.8, 137.2, 133.9, 132.9, 130.9, 130.8, 130.7, 130.2, 129.7, 125.8, 121.3, 68.1, 67.2, 52.7, 29.7, 15.0. ppm. $C_{91}H_{18}O_2S_2$, m/z calc. 1206.076, found 1206.072.

Synthesis of CCM_{60}-P. CCM_{60}-P was synthesized by reacting C_{60}-TM (50 mg, 0.04 mmol) with **CCM** (12 mg, 0.04 mmol) and tetrabromomethane (13 mg, 0.04 mmol) in 10 mL of *o*-DCB, was added DBU (2 drops) and stirred at room temperature. After 30 min the solution turned orange and CCM-$_{60}$P was the major product. The product was purified by column chromatography using a DCM:MeOH 30:1 mixture, as the eluent. ^{1}H-NMR (400 MHz; $CDCl_3$, 298 K); δ 7.85 (d, 2H), 7.46 (d, 4H), 7.19 (d, 4H), 6.87 (d, 2H), 4.34-4.48 (m, 16H) 2.50 (s, 6H), 1.31-1.43 (m, 24H) ppm. ^{13}C-NMR (100 MHz; $CDCl_3$, 298 K); δ 185.8, 163.9, 163.8, 148.5, 147.4, 146.9, 146.1, 145.0, 144.8, 144.5, 144.3, 144.3, 144.2, 143.9, 143.1, 142.2, 140.2, 139.9, 130.2, 129.5, 125.7, 121.7, 77.4, 77.0, 76.7, 72.5, 69.7, 69.7, 69.4, 69.3, 63.0, 62.9, 45.8, 45.2, 29.7, 15.0, 14.2, 14.1, 14.1ppm. $C_{109}H_{58}O_{64}S_2$, m/z calc. 1718.320, found 1718.328.

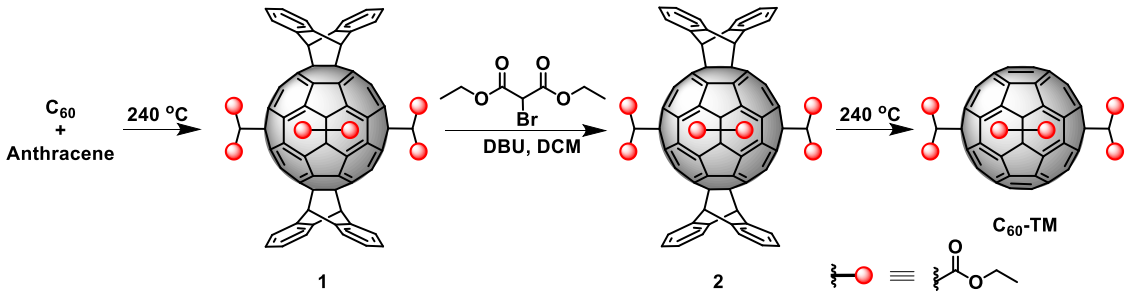

Scheme S2 Synthesis of C_{60}-TM.

Synthesis of C_{60}-TM. C_{60}-TM was synthesized following a procedure previously reported.[3]

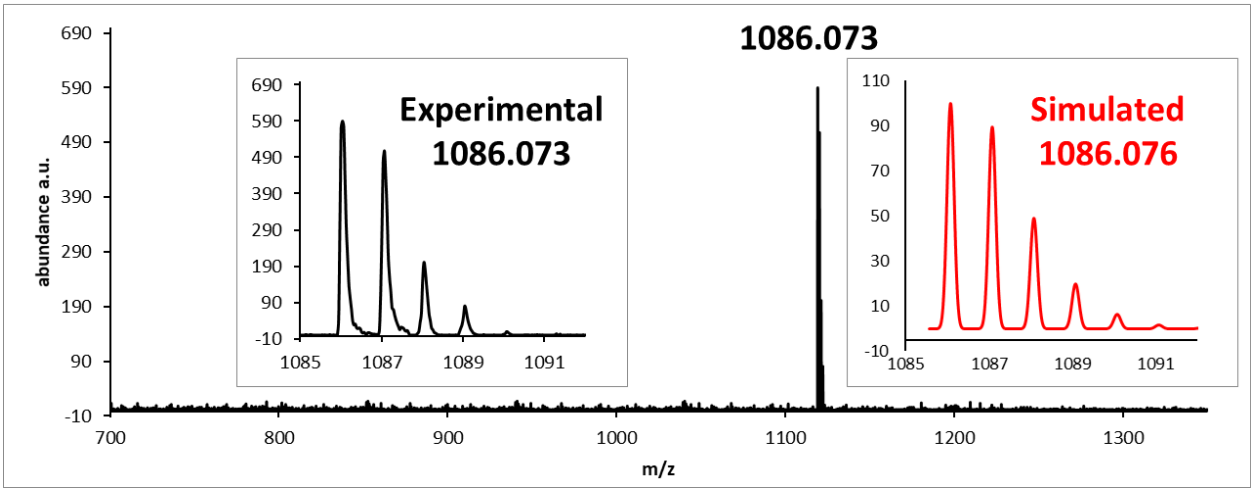

Figure S1. MALDI-TOF of CCM-C_{60}.

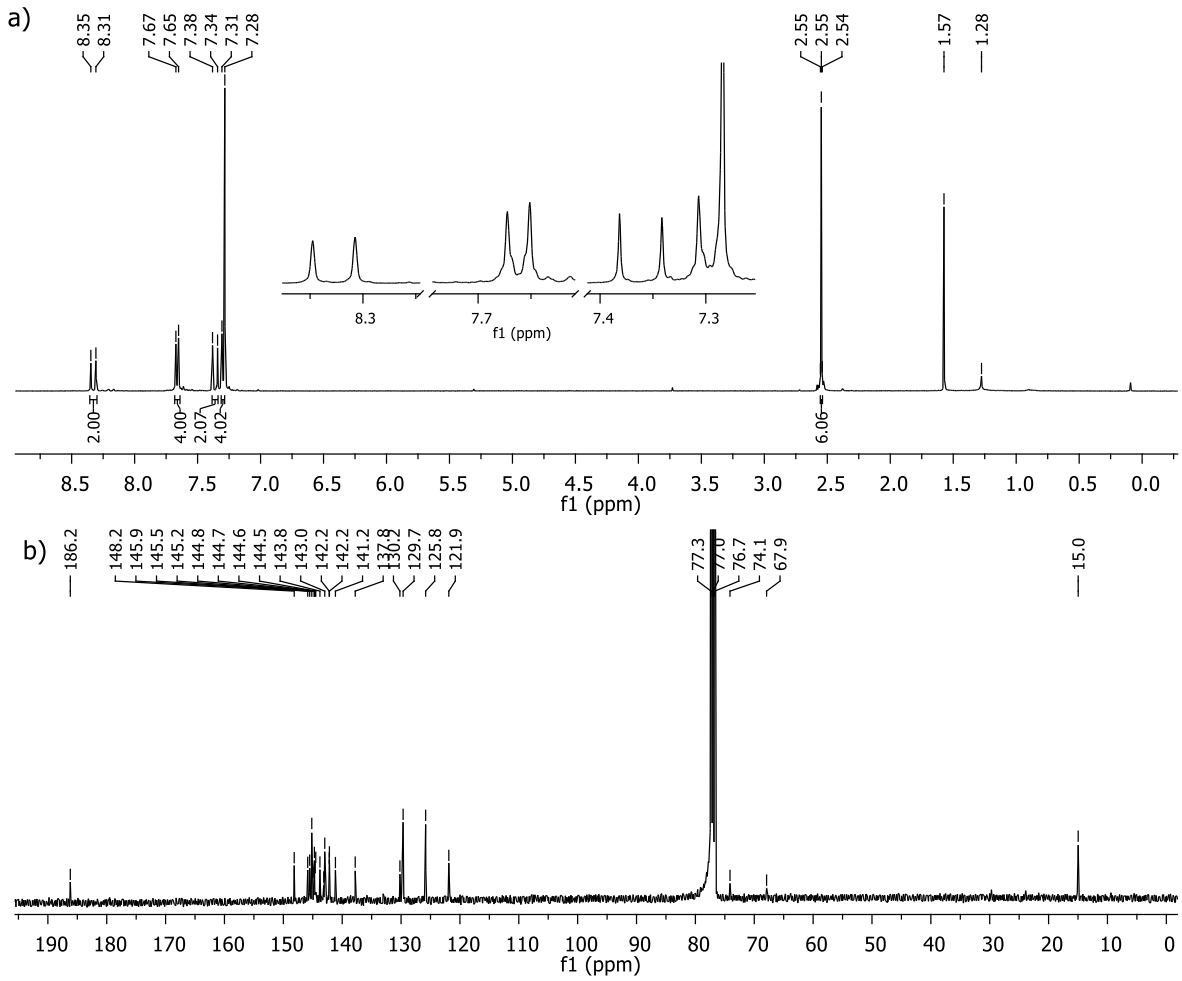

Figure S2. NMR spectra of CCM-C_{60} in $CDCl_3$, a) ^{1}H-NMR and b) ^{13}C-NMR.

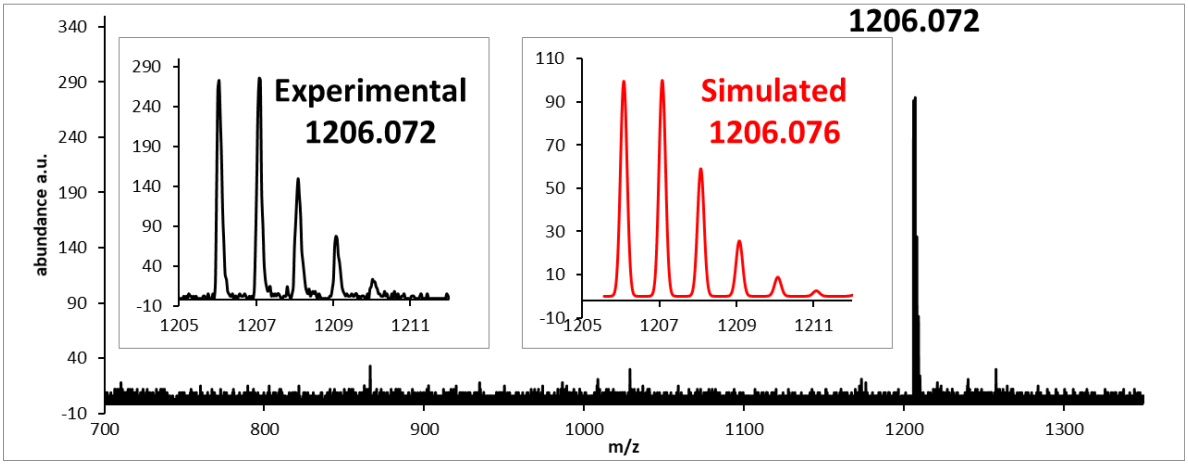

Figure S3. MALDI-TOF of CCM-C_{70}.

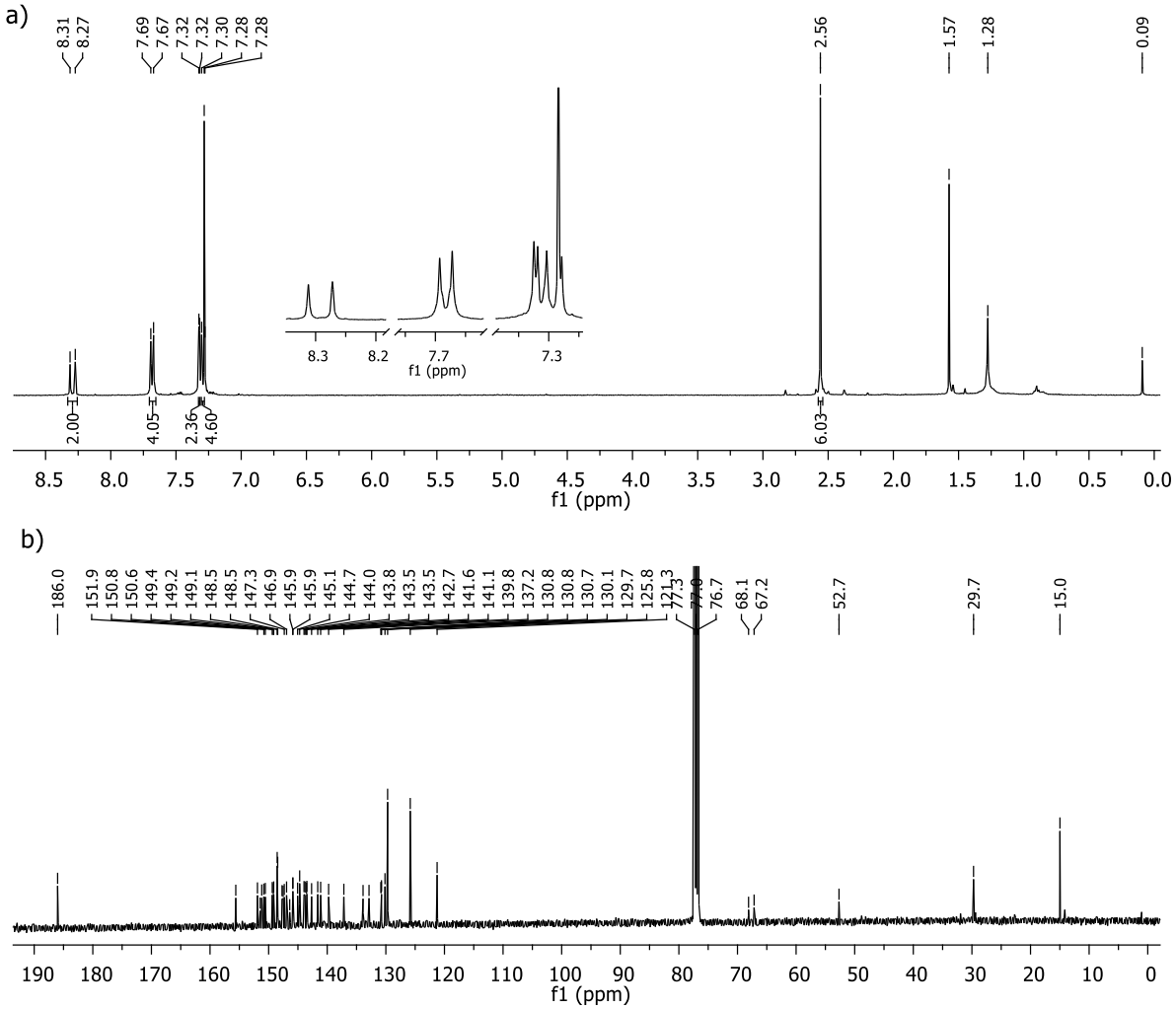

Figure S4. NMR spectra of CCM-C_{70} in $CDCl_3$, a) ^{1}H-NMR and b) ^{13}C-NMR.

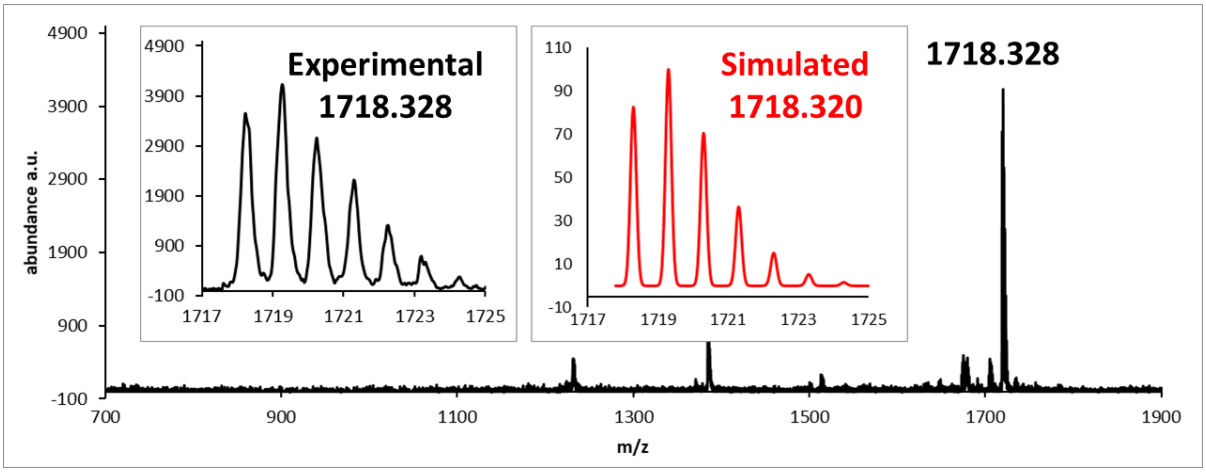

Figure S5. MALDI-TOF of CCM-C_{60}P.

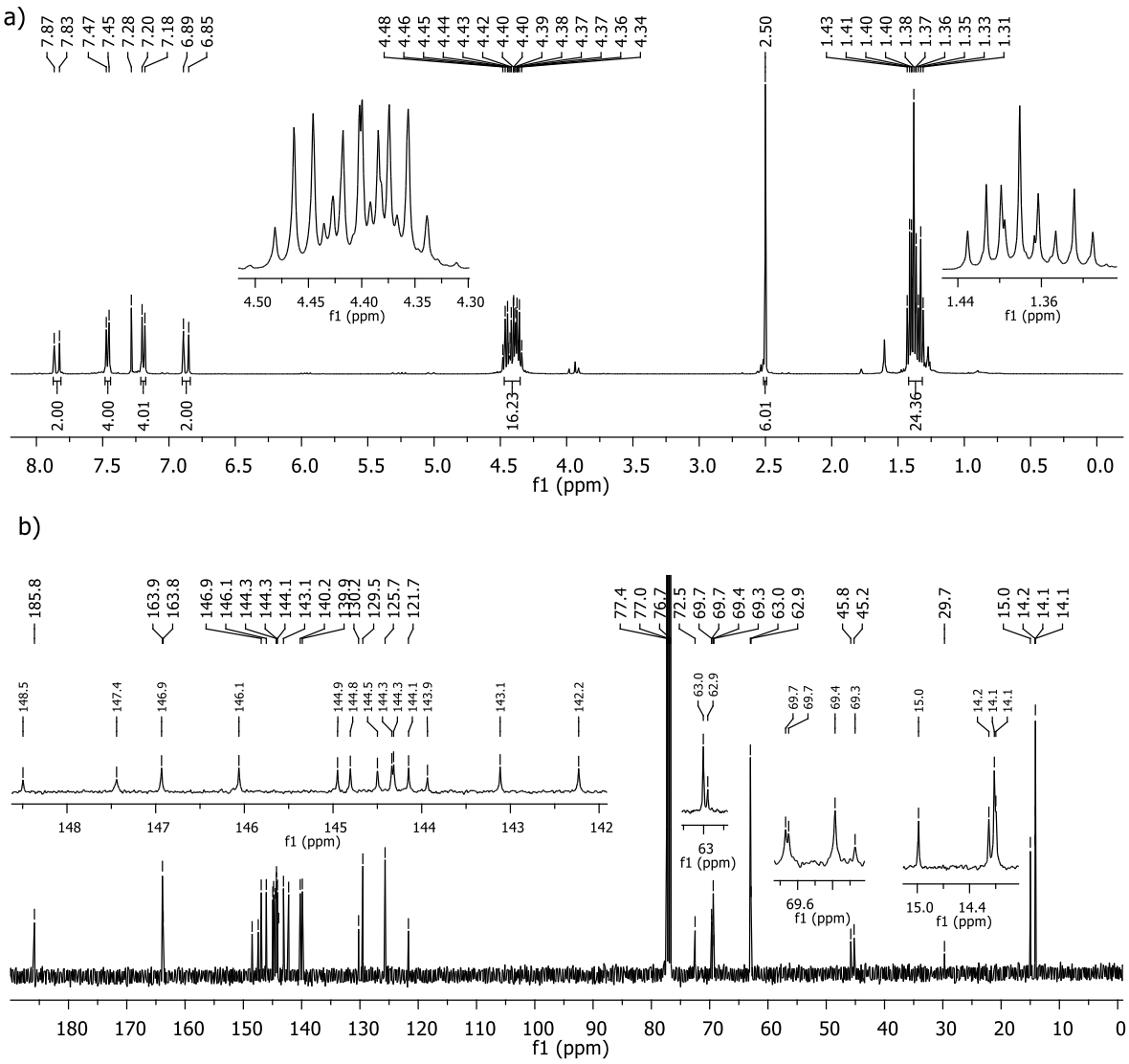

Figure S6. NMR spectra of C_{60}-TM in $CDCl_3$, a) ^{1}H-NMR and b) ^{13}C-NMR.

2. Filtering of conductance measurements

method I: A homemade MATLAB program is used to select traces that have high counts in the conductance region of interest. This filtering method is based on the fact that if a molecule is not trapped in the junction the conductance decreases exponentially; the corresponding breaking trace therefore, does not display many counts in the high-conductance region (insets of Fig. 2 a,c,e). To construct the 2D histogram in the main panels of Fig. 2a,c,e,g, we used the following criterion: traces with a number of counts, in the region defined from 1.1×10^{-6} G_0 to 2.5×10^{-4} G_0, higher than a factor of the average amount of counts in that region are selected, where this factor is 1.5, 1.5,0.9 and 1.1 for molecules CCM-C_{70}, CCM-C_{60}, CCM-C_{60}P and CCM, respectively. The insets in the same figure display the traces that did not satisfy this requirement and were therefore excluded from the selection. The sum of the two histograms constitutes the complete data set, which can be found in Fig. S7. The conductance values extracted with this approach from the corresponding one-dimensional conductance histograms are collected in Table 1.

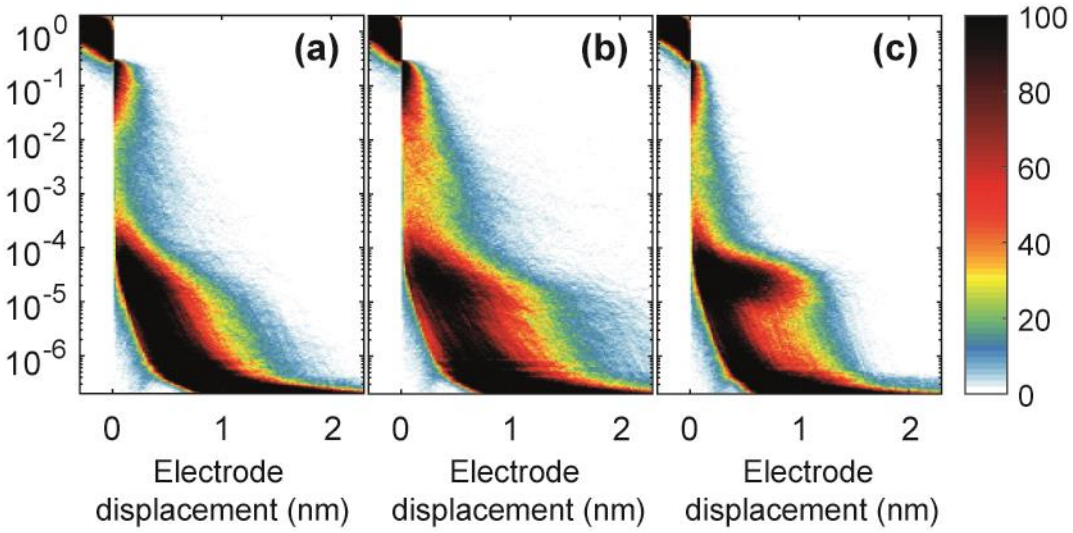

Figure S7. Two-dimensional conductance histograms built from 10.000 consecutive breaking traces recorded after drop-casting a solution containing CCM-C_{70} (a), CCM-C_{60} (b) and CCM-C_{60}P (c), respectively. The applied bias voltage is 100 mV and the measurement speed is 6.0 nm/s.

method II: unsupervised clustering method

The data was also filtered using the K-means++ clustering algorithm, following the methodology described in Ref. [4]. Briefly, the methodology is as follows: each breaking trace is converted into a 2D histogram with a resolution of 32x20 bins and into a 100-bin 1D histogram. This representation is combined to form the *feature space.* Each bin corresponds to one dimension in this space, and the position of each breaking trace is defined by the number of counts on each dimension. Then, the K-means++ algorithm is run 100 times with randomly initialized parameters to produce clusters with resembling breaking traces that yield the lowest cost function value. One-dimensional histograms are constructed for each cluster or class, from which the most probable conductance has been determined by log-normal fit; conductance values are reported in Table S1.

Table S1. Conductance values from the clustering analysis (method II). The two values in the yield correspond to the total yield and in parenthesis the yield considering molecular traces only. The length corresponds to the average plateau length of the traces in each class. For CCM molecule data are taken from Ref.2.

	Conductance Peak [G_0]	**Length [nm]**	**Yield (%)**
CCM			
class 1	4.8×10^{-5}	0.8	38 (100)
CCM-C_{70}			
class 1	1.4×10^{-5}	1.5	9 (74)
class 2	2.2×10^{-3}	0.5	1 (10)
class 3	7.6×10^{-2}	0.7	2 (16)
CCM-C_{60}			
class 1	1.4×10^{-5}	1.4	11 (52)
class 2	4.6×10^{-6}	0.9	3 (14)
class 3	2.7×10^{-3}	0.5	7 (34)
CCM-C_{60}P			-
class 1	2.6×10^{-5}	1.2	34 (79)
class 2	2.8×10^{-5}	0.6	9 (21)

In Figs. S8 – S11, the results of the clustering analysis for the four molecules are presented. For CCM, only 2 classes are found, with class 2 being the empty class, where no molecular signature is observed. For CCM-C_{60} and CCM-C_{70} four classes were found, while for CCM-C_{60}P three different classes were found. The corresponding 2D and 1D conductance histograms are displayed in Figs. S8 – S11.

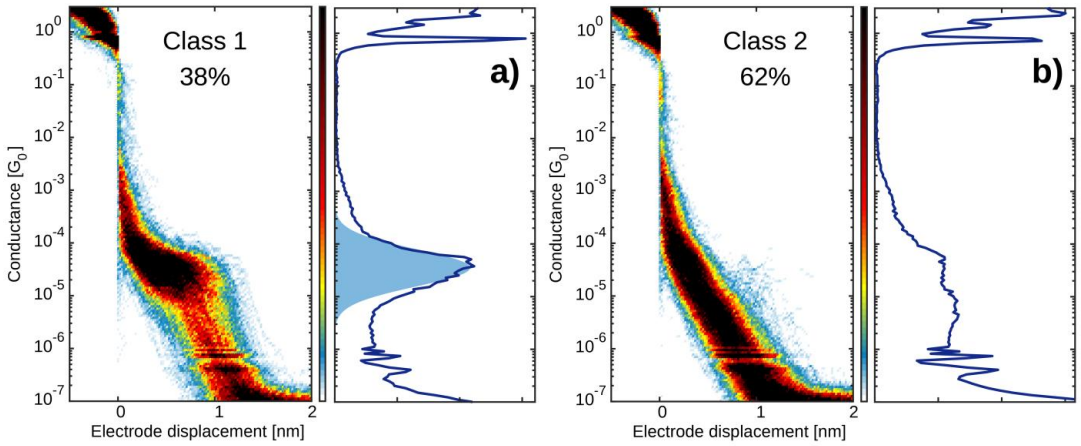

Figure S8. 2D and 1D histograms filtered with the clustering method for the free CCM (data from Ref. 2). Two classes are found: class 1 (a)) presents the molecular traces whereas class 2 (b)) corresponds to traces without clear molecular signature. In the figure the yield of each class is indicated.

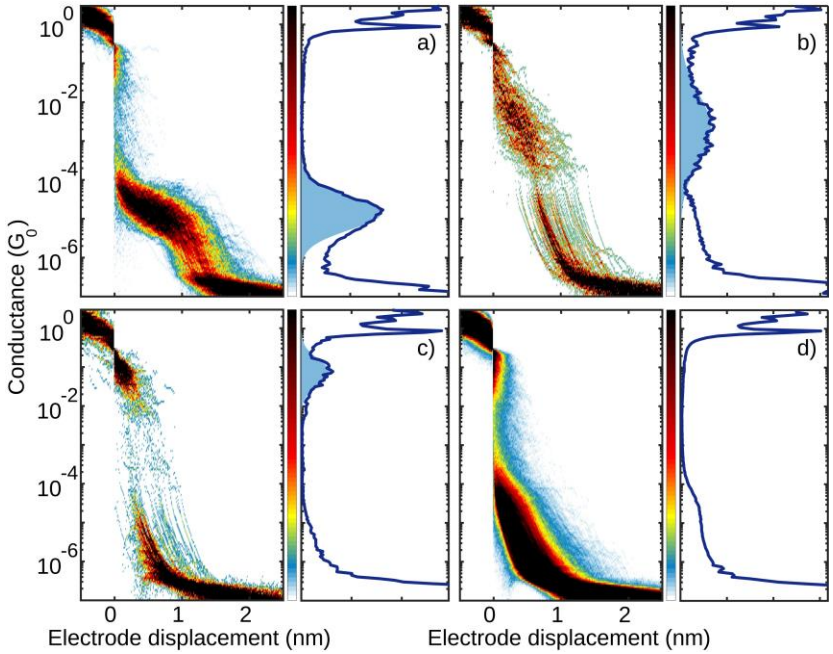

Figure S9. 2D and 1D histograms from the measurements of CCM-C_{70} using the clustering method (method II) for a) class 1 (9% of the total traces), b) class 2 (1%), c) class 3 (2%) and d) class 4 corresponding to traces without a clear molecular signature.

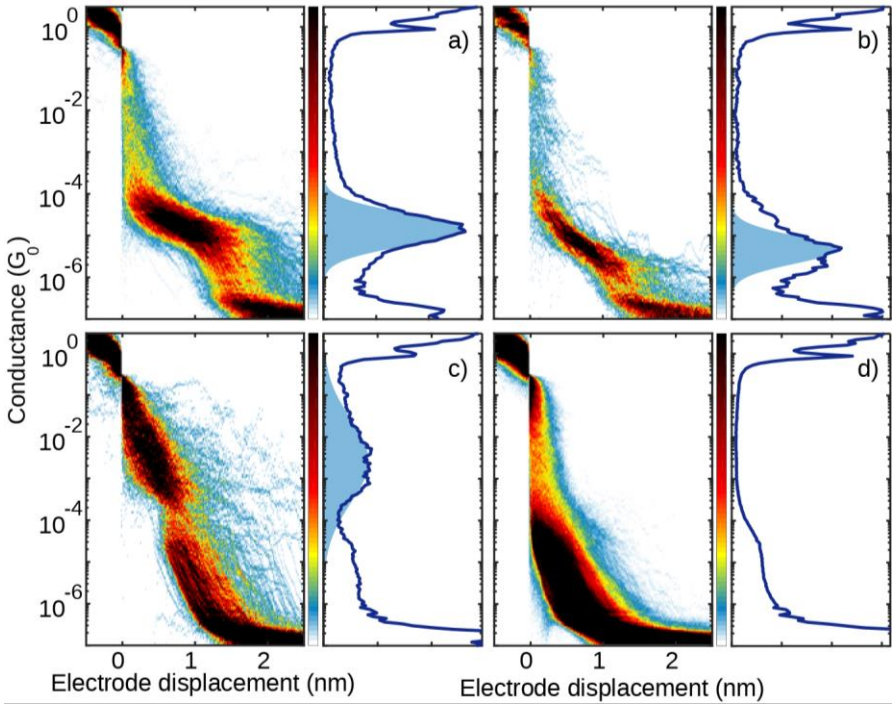

Figure S10. 2D and 1D histograms from the measurements of CCM-C_{60} using the clustering method (method II) displaying a) class 1 (11% of the total traces), b) class 2 (3%), c) class 3 (7%) and d) class 4 corresponding to traces without a clear molecular signature.

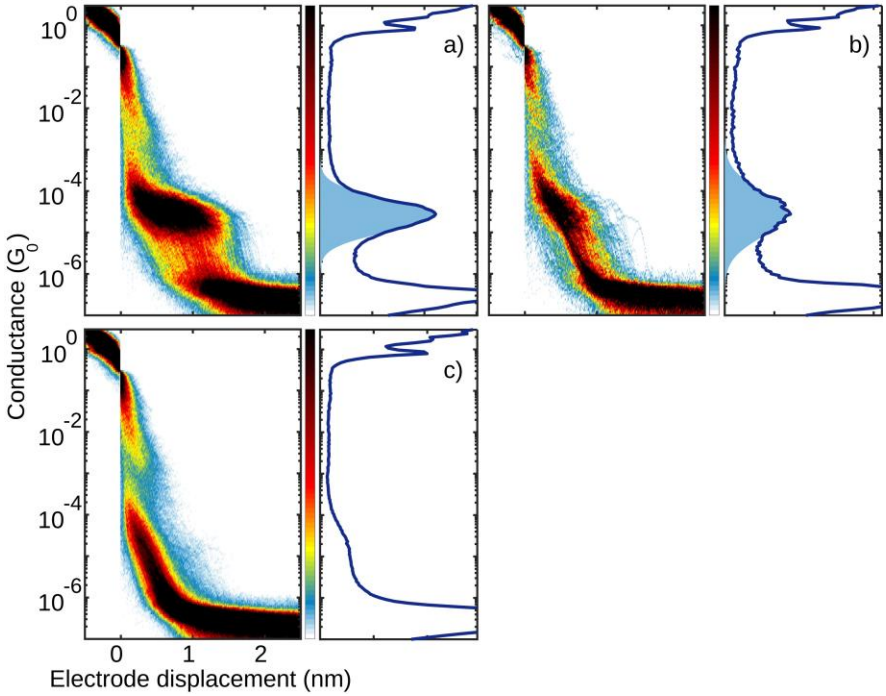

Figure S11. 2D and 1D histograms from the measurements of CCM-C_{60}P using the clustering method (method II) displaying a) class 1 (11% of the total traces), b) class 2 (3%) and c) class 3 corresponding to traces without a clear molecular signature.

In Fig. S12 example of single traces for the case of CCM-C_{60}, CCM-C_{70} and CCM-C_{60}P are shown to compare the behavior of the most prominent class (class 1). Although the three molecules present the same conductance, the single traces of CCM-C_{60}P are flat, while for the other two molecules the traces present a more slanted step in agreement with a sliding process of the electrode on the surface of the fullerene.

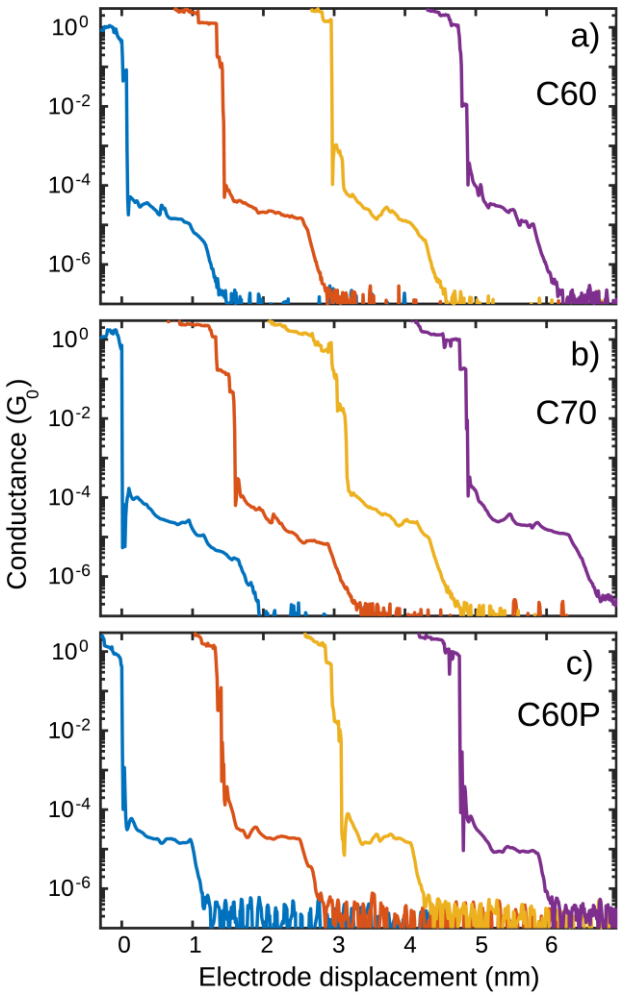

Figure S12. Examples of single breaking traces for class 1 of a) CCM-C_{60}, b) CCM-C_{70} and c) CCM-C_{60}P. A horizontal offset was used for clarity.

In Fig. S13 example breaking traces from class 3 of CCM-C60 are shown. As can be seen, these traces do not present a clear plateau but show a *downhill* behaviour with small steps at different conductance values.

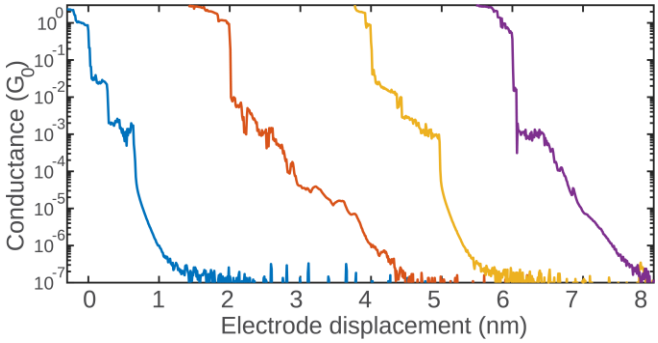

Figure S13. Example of single traces with high conductance peaks for the case of CCM-C_{60} (class 3). A horizontal offset was used for clarity.

Finally, in Fig. S14 the control measurements are shown. As a general rule, for the measurement of these molecules, the bare gold was measured for more than 2000 traces before depositing the molecule, followed by 1000 traces after drop-casting the solvent only (dichloromethane DCM). Thus, only if the sample present clean control measurements the molecules are drop-casted. In Fig. S14 the last 2000 traces of gold, the 1000 traces of DCM and the first 2000 traces of the molecule are presented side by side in five histograms of 1000 traces each. As can be seen, the molecular feature appears abruptly just after drop casting the molecule.

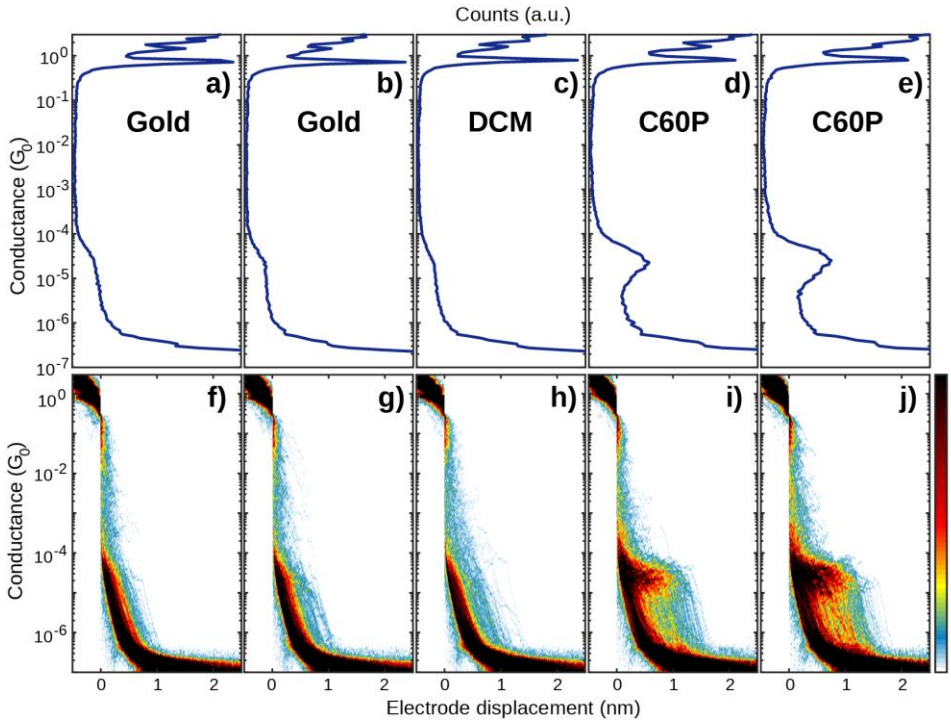

Figure S14. Control measurements. 2D and 1D histograms of 1000 consecutive traces each, showing a), b), f), g) the last 2000 traces of the bare gold measurements c), h) the 1000 traces of the subsequent dichloromethane solvent measurement (DCM) and d), e) ,i) ,j) the first 2000 traces of the drop-casted molecule (CCM-C_{60}P).

3. Additional results theoretical analysis

Two types of calculations were performed related to: (i) discrete molecules and systems with finite electrodes that were carried out with Gaussian09 and ORCA 4.0.1, respectively using the hybrid B3LYP functional and(ii) the molecular device setup, featuring periodic boundary conditions, that were calculated using the ATK code with the PBE functional.

In a previous study,[5] a comparison is made between a non-hybrid functional PBE, two hybrid functionals B3LYP and TPSSh and a long-range corrected one, wB97X. The two hybrid and the long-range corrected functionals yield a large gap thereby correcting for the well-known drawback of the PBE functional. However, the gap of wB97X is larger than the one found with the other two hybrid functionals. In order to check the accuracy of the different approaches, we have calculated the isolated molecules studied in this paper and for the CCM molecule wB97X gives a HOMO-LUMO difference of 7.58 eV (163 nm) while the B3LYP value is 3.4 eV (360 nm). In Ref. [2], we show the UV spectra for the CCM in the solid state displaying a maximum at 420 nm, clearly in better agreement with the B3LYP value. For this reason, the results in this paper using non-periodic approaches have been calculated at the B3LYP level. It is worth to remark that the composition of the frontier orbitals is the same in the tested exchange correlation functional only the orbital energies show important differences. Thus, the nature of the transport channels is the same one.

It is worth to remark that the exchange-correlation functional changes the energy, but the shape of the orbitals is very similar. Furthermore, in Fig. 3 not the orbitals of the molecule but the transmission eigenfunctions are given which give a much better representation of the transport channels than the orbitals. Furthermore, such transmission eigenfunctions cannot be obtained with hybrid functionals; they are not implemented in any code with hybrid functionals. Thus, we plot them with the PBE functional, and we represented the energies of the levels with different functionals in the transmission curves.

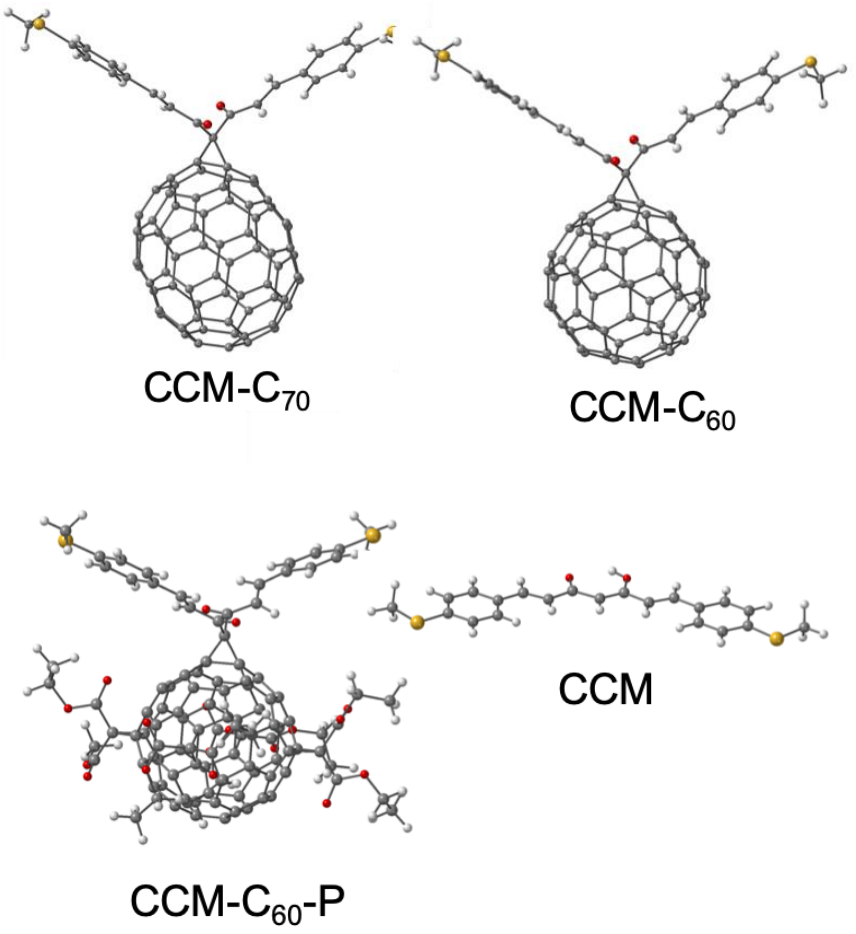

Figure S15. Optimized structures at DFT level of the CCM-C_{70}, CCM-C_{60}, CCM-C_{60}P and CCM molecules. The terminal Me-S groups adopt a coplanar conformation in the isolated optimized molecules.

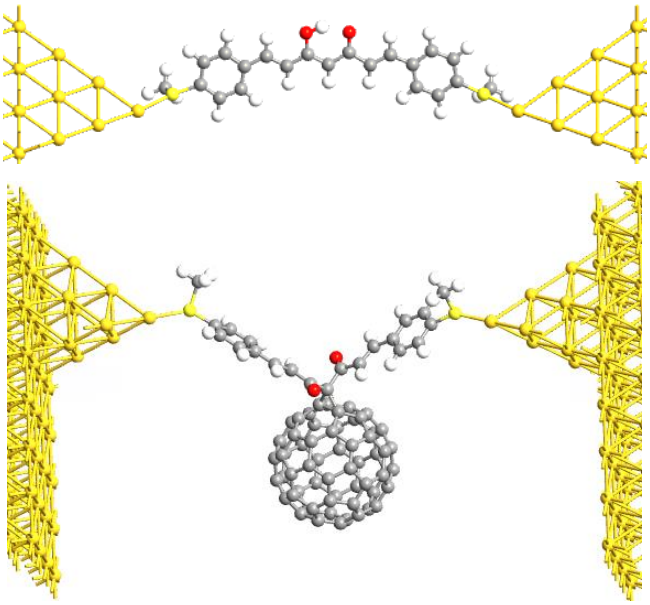

Figure S16. Structures of the CCM and CCM-C_{60} attached to the gold electrodes employed in the transport calculations. The terminal Me-S groups adopt a perpendicular conformation in the isolated optimized molecules.

Table S2. Calculated conductance values (in G_0 units) obtained with the ATK code using full consistent NEGF method and the PBE functional for different conformers of the five studied molecules. Two orientations of the methyl groups were considered from the geometry optimizations: coplanar (as in isolated molecules, see Fig. S15) or perpendicular (when the molecules are sandwiched between the electrodes, see Fig. S16). The conductance values were calculated using the intensity value obtained with the experimental bias (100 mV) assuming lineal I/Vdependence.

	coplanar	perpendicular
CCM-C_{70}	9.6×10^{-4}	2.2×10^{-3}
CCM-C_{60}	6.1×10^{-4}	1.7×10^{-3}*
CCM	3.5×10^{-3}	4.4×10^{-3}

* The same conductance was obtained for a model of a V-shaped CCM-C_{60} where the fullerene was replaced by two hydrogen atoms.

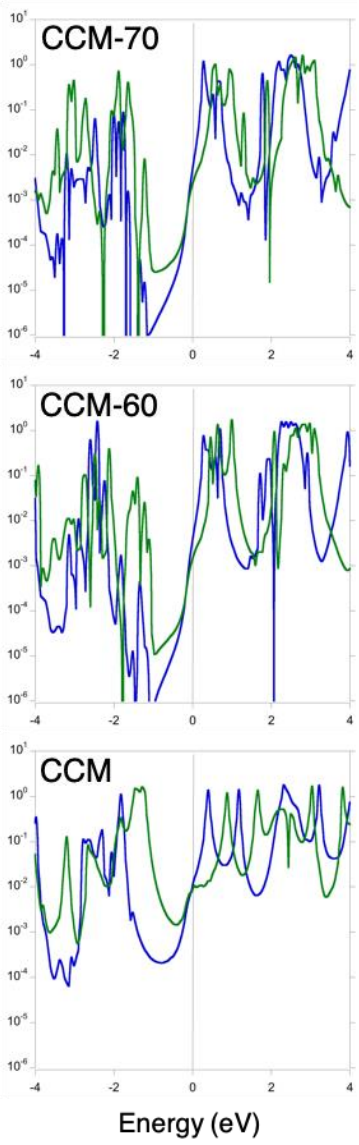

Figure S17. Transmission curves for systems based on the CCM-C_{70} CCM-C_{60} and CCM molecules calculated with the ATK code and PBE functional with perpendicular (blue) and coplanar (green) orientations of the methyl substituents of the methylthio anchoring groups.

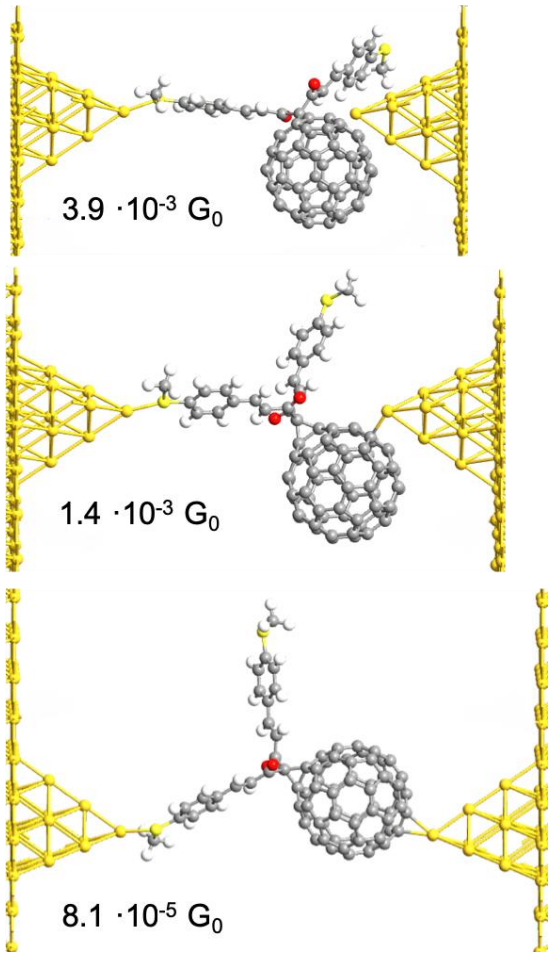

Figure S18. Optimized structures using the GFN-xTB approach for the sliding process of the gold electrode on the surface of the fullerene of the CCM-C_{60} molecule and the calculated conductance values with the ATK code and PBE functional.

References

[1] Castro, E.; Cerón, M. R.; Garcia, A. H.; Kim, Q.; Etcheverry-Berríos, A.; Morel, M. J.; Díaz-Torres, R.; Qian, W.; Martinez, Z.; Mendez, L.; Perez, F.; Santoyo, C. A.; Gimeno-Muñoz, R.; Esper, R.; Gutierrez, D. A.; Varela-Ramirez, A.; Aguilera, R. J.; Llano, M.; Soler, M.; Aliaga-Alcalde, N.; Echegoyen, L. A new family of fullerene derivatives: fullerene-curcumin conjugates for biological and photovoltaic applications. *RSC Adv.* **2018,** *8*, 41692-41698.
[2] Olavarría-Contreras, I. J.; Etcheverry-Berríos, A.; Qian, W.; Gutiérrez-Cerón, C.; Campos-Olguín, A.; Sañudo, E. C.; Dulić, D.; Ruiz, E.; Aliaga-Alcalde, N.; Soler, M.; van der Zant, H. S. J. Electric-field induced bistability in single-molecule conductance measurements for boron coordinated curcuminoid compounds. *Chem. Sci.* **2018,** *9*, 6988-6996.
[3] Castro, E.; Azmani, K.; Hernandez Garcia, A.; Aghabali, A.; Liu, S.; Metta-Magana, A.; Olmstead, M.; Rodriguez-Fortea, A.; Poblet, J.; Echegoyen, L. Unusual C2h-symmetric trans-1-(bis-pyrrolidine)-tetra-malonate hexa-adducts of C60. The unexpected regio- and stereo-control mediated by malonate-pyrrolidine interaction. *Chem. Eur. J.* **2017,** *23*, 15937-15944.
[4] Cabosart, D.; El Abbassi, M.; Stefani, D.; Frisenda, R.; Calame, M.; van der Zant, H.S.J.; Perrin, M.L.; A reference-free clustering method for the analysis of molecular break-junction measurements. *Appl. Phys. Lett.* **2019**, *114*, 143102.
[5] Martín-Rodríguez, A.; Aravena, D.; Ruiz, E. DFT Approaches to Transport Calculations in Magnetic Single-Molecule Devices. Theor. Chem. Acc. **2016**, *135* (8), 192.

Optimized geometries at B3LYP/6-311G* level with Gaussian09

CCM-C_{70}

C	-13.02062600	4.60113600	-2.33902300
C	-12.87291800	9.91443100	-6.84697200
C	-11.59515300	8.69953500	-0.10623300
C	-14.51041100	5.55417800	-6.46272600
C	-15.19881700	5.40637600	-2.42794300
C	-13.66088800	7.62891600	-7.48048900
C	-14.90343300	11.40434700	-2.94082400
C	-10.71562700	5.21842400	-4.95557100
C	-10.86280200	5.91312100	-6.14653500
C	-14.44281700	11.07535200	-5.32282800
C	-14.26663000	4.50432300	-3.06655200
C	-9.91856100	9.82574400	-1.51929000
C	-10.04216200	7.47569400	-1.54892000
C	-10.36096800	7.26446800	-6.25148000
C	-16.50577900	8.24682100	-4.08860100
C	-15.68373000	7.71593400	-6.33654700
C	-15.39139600	10.02298200	-5.41769100
C	-12.10281500	5.82597400	-6.88901300
C	-9.27692200	9.33286600	-2.74077800
C	-11.93669900	11.01046400	-0.83282800
C	-11.79943600	4.39978300	-4.45703100
C	-12.20043700	11.72447100	-5.24334000
C	-15.65545200	9.54290500	-1.75588500
C	-12.86930700	11.77222900	-1.63233100
C	-12.12640100	6.35571300	-0.79823100
C	-13.92559400	9.01162800	-7.14477300
C	-15.19449500	5.13254900	-5.25581300
C	-10.73541700	5.43758400	-2.63607500
C	-15.17003500	9.06581000	-6.43936000
C	-9.47989700	7.13793800	-3.93816700
C	-9.39043200	10.01585200	-3.93095300
C	-11.28486200	8.02089600	-7.04419200
C	-16.09263700	9.59921900	-4.19869200
C	-9.36388400	7.88775500	-2.73905900
C	-13.19927900	11.02593100	-6.02775800
C	-14.21258400	11.39271600	-1.68255400
C	-13.77306400	9.49860700	-0.18716400
C	-14.53745400	6.03331200	-1.30115500
C	-11.81417700	4.55054100	-3.01774700
C	-16.35917600	7.52211700	-2.86200100
C	-10.58597000	10.04082000	-5.92959300
C	-16.33629400	7.31355700	-5.18284300
C	-9.64061300	7.86800700	-5.19176600
C	-12.48979800	7.55996900	-0.14633100
C	-12.38447800	9.89882300	-0.11493500

C	-13.19443400	5.53870900	-1.24931400
C	-16.09355800	5.99833700	-4.63298100
C	-9.66342700	9.28574900	-5.13845900
C	-15.79613500	8.13130800	-1.71301700
C	-11.50895300	9.39706400	-6.79357100
C	-10.85022800	6.30840500	-1.52334700
C	-14.75650300	6.81949800	-6.99265100
C	-14.25996800	4.36823200	-4.45480400
C	-10.66458400	10.99379200	-1.50783800
C	-10.39549400	8.66156700	-0.80387700
C	-12.18745400	12.23928100	-2.81020000
C	-13.83363800	8.05343500	-0.19382100
C	-15.79987800	10.26662600	-2.98368100
C	-16.09225300	6.13682500	-3.19363100
C	-12.84806100	12.22058100	-4.02658300
C	-14.66668600	10.22888200	-0.95335400
C	-14.84814000	7.35650400	-0.90096100
C	-12.36371100	7.14171900	-7.43433300
C	-14.22813500	11.79561900	-4.08927900
C	-10.05903500	5.84772500	-3.82927700
C	-10.90496800	11.25433600	-5.22659300
C	-13.15221100	5.04633800	-6.40943400
C	-12.99699100	4.31603900	-5.16525400
S	-6.66804200	16.87335400	-11.24562200
S	-6.09301800	16.18243800	4.67304600
O	-10.64391300	14.74380800	-3.56509600
O	-7.28302400	12.07387400	-3.13680500
C	-6.93642500	14.13001900	0.64203700
C	-7.11570100	13.44921200	-0.62721500
H	-6.24247700	12.93473100	-1.02452700
C	-8.60855000	15.56539700	-7.28339200
C	-7.96730000	14.82212900	1.30083500
H	-8.95757700	14.86799700	0.86132000
C	-5.67318800	14.10263300	1.26305000
H	-4.85625600	13.57499500	0.78016900
C	-9.87049700	13.93829600	-4.04582900
C	-9.27286000	15.22904300	-6.03725800
H	-10.00592700	15.94736400	-5.67434600
C	-6.48786700	15.41737200	3.12243900
C	-9.09873300	14.12851600	-5.27740300
H	-8.40129400	13.34063600	-5.54027000
C	-8.24572100	12.62030900	-2.63324000
C	-5.44829300	14.73069400	2.47512300
H	-4.46248400	14.68956400	2.92739500
C	-7.75280800	15.45413500	2.51530000
H	-8.57824900	15.97374600	2.98448200
C	-8.23666000	13.36892000	-1.37310900
H	-9.16839500	13.84051600	-1.08031500

C	-7.37300800	16.30824500	-9.71932700
C	-9.60660400	12.60025600	-3.34117400
C	-7.63450400	14.74986500	-7.88488500
H	-7.34289000	13.81661400	-7.41599300
C	-8.34444400	17.13286300	-9.12983000
H	-8.62715700	18.06468000	-9.60925800
C	-8.94518000	16.76496600	-7.93898300
H	-9.69432100	17.41703800	-7.50009700
C	-7.02648100	15.10906500	-9.07724000
H	-6.28193400	14.44764400	-9.50130700
C	-5.46839900	15.57112300	-11.67216300
H	-4.69188100	15.47873000	-10.91232900
H	-5.00858500	15.89183600	-12.60688500
H	-5.95933100	14.61103400	-11.83397100
C	-7.66724700	16.93629000	5.19410200
H	-7.99975300	17.69855000	4.48884500
H	-7.46015200	17.41182800	6.15273600
H	-8.44341000	16.18370000	5.33582500
C	-10.01976800	11.35001000	-4.04129000
C	-10.74493500	11.91815100	-2.67066200

CCM-C_{60}

S	0.22932200	9.22250800	8.26400800
S	15.87916900	11.34916600	10.71286800
O	8.44856300	5.79997700	8.16918400
O	9.16736500	8.99740200	5.36456500
C	12.42120000	9.90451900	8.04316200
C	11.33174600	9.53385100	7.15865400
H	10.97373900	10.31175100	6.48654200
C	4.51013200	7.55482800	8.00045500
C	13.01109600	9.01699600	8.95955400
H	12.65264900	7.99626100	9.03447600
C	12.93052500	11.21603800	7.99028200
H	12.49711300	11.92524900	7.29161900
C	8.10782000	6.47532800	7.21722800
C	5.84395300	6.98158700	7.99513400
H	6.09157600	6.33323000	8.83382400
C	14.55160600	10.72467400	9.71622000
C	6.81277600	7.14737700	7.07181200
H	6.68247700	7.76628800	6.19076600
C	9.63601600	8.13633500	6.08479500
C	13.97155300	11.62229200	8.80585100
H	14.34200300	12.64026200	8.73819700
C	14.05435800	9.41374800	9.78108800
H	14.47656700	8.69427300	10.47078700
C	10.71321000	8.33942700	7.05831300
H	10.98492200	7.48672500	7.67106200
C	1.88863400	8.61744800	8.09911200

C	9.07212500	6.71110500	6.04764700
C	4.03340200	8.41282200	6.99454100
H	4.67317400	8.67905700	6.16041600
C	2.35149000	7.76153800	9.11110000
H	1.70115000	7.50212100	9.94047900
C	3.63392800	7.24486700	9.05789800
H	3.97200000	6.58410000	9.85040800
C	2.75087600	8.93604100	7.03844400
H	2.42948300	9.59250000	6.24020400
C	0.00813800	10.27656800	6.79503900
H	0.70917200	11.11170600	6.79260800
H	-1.00588200	10.66966600	6.86748200
H	0.09671700	9.70211500	5.87246400
C	16.38526100	9.90993200	11.70814900
H	15.58102100	9.57008900	12.36139500
H	17.21406600	10.25827000	12.32438400
H	16.73552000	9.09190800	11.07797700
C	7.08568500	4.01770700	0.95912300
C	6.73325200	4.18933700	2.35745900
C	6.68064000	2.88769600	2.97619600
C	7.00066500	1.89805600	1.96421800
C	7.25268100	2.59731600	0.71606800
C	7.92574400	4.93511500	0.33633300
C	8.97076000	4.47386900	-0.55777700
C	10.13430100	5.32048000	-0.35838600
C	9.80593800	6.30255100	0.65819400
C	8.44932300	6.06391300	1.08462600
C	7.24166400	5.26834800	3.07834200
C	8.11697800	6.22487200	2.42894200
C	9.09212600	6.67869700	3.38692200
C	8.72444100	6.12829500	4.71861500
C	7.66461200	5.11646700	4.44830500
C	7.14166500	2.72958300	4.28391200
C	7.64787800	3.86285000	5.03259600
C	8.77525500	3.38493200	5.85422100
C	8.93882600	1.97121700	5.59060500
C	7.93287200	1.56427600	4.62857700
C	7.76143100	0.78152300	2.29951900
C	8.23227100	0.60827100	3.66234800
C	9.55980600	0.02172500	3.60774900
C	9.91389400	-0.15498000	2.21330400
C	8.80135800	0.31460300	1.40393500
C	8.25524400	2.15227100	-0.14215800
C	9.04555700	0.98741900	0.20890100
C	10.41074300	1.22350600	-0.22543200
C	10.46400200	2.53680200	-0.84282800
C	9.13240100	3.11050900	-0.79231500
C	11.57931700	3.34961400	-0.65379800

C	12.69119600	2.88029900	0.15561300
C	13.20890300	4.00866900	0.90385200
C	12.41254600	5.17466600	0.56411500
C	11.41086800	4.76759600	-0.40550600
C	12.09232600	6.10811500	1.54563500
C	12.56013400	5.92793100	2.90633900
C	11.52868400	6.39737600	3.80979800
C	10.40101300	6.87539500	2.98758600
C	10.76319200	6.68599100	1.59890200
C	11.31523500	5.73672900	5.00602900
C	12.07736200	4.55209500	5.31125700
C	11.20237300	3.59581800	5.96078900
C	9.88827500	4.17572500	6.06965000
C	9.97123500	5.59594600	5.63385400
C	11.37098000	2.23102200	5.73177600
C	12.41725200	1.76709300	4.83826100
C	11.89421700	0.63764800	4.09304900
C	10.52777600	0.40912400	4.52999100
C	10.21008100	1.39665200	5.54467900
C	12.23389500	0.47318200	2.75227700
C	13.11085400	1.43196700	2.10217200
C	12.64123400	1.61820200	0.74233400
C	11.47562300	0.77436200	0.55016000
C	11.22342000	0.06780300	1.79314400
C	13.61218600	2.51536800	2.81961000
C	13.66102700	3.83225100	2.20834100
C	13.33546900	4.81253600	3.22754100
C	13.08679300	4.10609100	4.46008500
C	13.25739500	2.68486500	4.21607200

CCM

S	9.36975146	5.15784710	17.77708709
S	0.56167500	2.83251100	1.65177100
O	8.50628063	5.75938424	8.97308283
O	7.26101509	5.42531947	6.75847795
H	7.97513488	5.69212350	7.40249707
C	3.91050201	4.08076832	4.56257616
C	5.02024775	4.51123114	5.40221858
H	5.85352400	4.97364683	4.88006651
C	8.76885491	5.39346870	13.21555731
C	2.74861178	3.46473661	5.05629919
H	2.63946478	3.28367714	6.12030622
C	3.98725324	4.28547896	3.17207365
H	4.87147221	4.75843360	2.75548285
C	7.54048708	5.22371602	9.56697146
C	8.59588585	5.47760095	11.77175323
H	9.41117369	5.93909311	11.21835913

C	1.81148000	3.28561400	2.83099000
C	7.55301948	5.05733675	11.03194342
H	6.68514484	4.58409698	11.48142989
C	6.28850613	4.87077998	7.47837005
C	2.96526091	3.89896023	2.32178713
H	3.05911275	4.07207915	1.25430740
C	1.71812446	3.07395640	4.21333685
H	0.84233485	2.60408549	4.64335036
C	5.13030535	4.40284243	6.74195839
H	4.34544330	3.95426048	7.34204834
C	9.21278182	5.28597066	16.01209781
C	6.38183770	4.75090306	8.84955349
H	5.56381643	4.29249054	9.39062542
C	7.81831507	4.82198366	14.08488618
H	6.89629509	4.41212226	13.68706751
C	10.16662102	5.85592060	15.16458070
H	11.08848750	6.26485342	15.55877899
C	9.94046942	5.90432064	13.79317953
H	10.69365570	6.35101491	13.15093681
C	8.03246336	4.76847535	15.44871751
H	7.28129542	4.32188733	16.09286225
C	10.98876111	5.91344780	18.12342517
H	11.79993043	5.36371536	17.64557411
H	11.11298224	5.85088298	19.20444162
H	11.01434174	6.96269588	17.82845976
C	1.25668809	3.36315461	0.05572517
H	1.41590929	4.44120903	0.02429230
H	0.50597706	3.09901118	-0.68903123
H	2.18100465	2.83424999	-0.17754386